

Causality Relation Map: A Novel Methodology for the Identification of Hierarchical Fibrillatory Processes

M Rodrigo, A Liberos, MS Guillem, J Millet, AM Climent

BioITACA, Universitat Politecnica de Valencia, Valencia, Spain

Abstract

Cardiac fibrillation is a complex arrhythmia whose mechanisms of onset, maintenance and interruption are not completely understood. Fibrillatory processes have usually been considered as random phenomena without any apparent coordinated pattern. However, recently developed experimental and human studies have demonstrated that a hierarchical activation may govern some fibrillatory processes. In this study a novel methodology for the identification of hierarchical activation patterns is presented. Specifically, causal relations between neighboring electrodes are used to identify predominant propagation directions. The presented methodology may be of useful to identify regions of the myocardium that may sustain a fibrillatory process and consequently are targets for arrhythmia termination.

1. Introduction

Fibrillation is a complex and self-sustained arrhythmia which makes the myocardium completely inefficient in its mechanical functions. This inefficiency can cause serious health problems in case of taking place in the atria and, in case of ventricular fibrillation, the arrhythmia can rapidly provoke death if it is not halted on time.

The multiple wavelet hypothesis postulates that fibrillation is the result of the random propagation of multiple wavelets across the atria [1]. However recent, clinical studies have revealed the existence of a hierarchical organization in the rate of activation of different regions in the atria [2]. According to this hierarchical organization theory, it is possible to identify areas of tissue responsible for the onset and/or maintenance of the arrhythmia. Identification of these hierarchical patterns in patients may be useful for the application of therapeutic strategies, such as radiofrequency ablation. Additionally, analysis of the changes induced by drugs or manoeuvres that alter the electrophysiological properties of the myocardium may be of importance for developing novel therapies.

In order to identify the hierarchical pattern of electrical

activation of a myocardial tissue, we make use of causality relations. One possible definition of causality was given by Clive Granger, Nobel Prize for Economics: "If a signal $x(t)$ is useful for predicting future values of $y(t)$, then $x(t)$ is cause of $y(t)$ ". By applying the concept of causality to the signals obtained from the myocardium it is possible to establish the hierarchical relationship between the areas from which the signal preferably comes, and thus obtain the global hierarchical pattern.

2. Database

The database comprises simulated electrograms and real recordings from Optical Mapping experiments in isolated hearts during fibrillation.

2.1. Mathematical models

A 2-D model of human atrial tissue was used [3] (250x250 cells separated by 0.1mm). Euler integration method was applied to solve the differential equations with a time interval of 0.005ms. Four different propagation patterns were simulated: a focal pattern; a rotatory propagation pattern; a rotatory propagation pattern in a non-uniform tissue simulating left and right atria; and a random focal propagation pattern. From each mathematical simulation, a squared mesh of 11x11 pseudo-unipolar electrograms were calculated under the assumption of a homogenous, unbounded and quasi-static medium by using the following expression:

$$\text{Unipolar electrogram} = \sum_{\vec{r}} \left(\frac{\vec{r}}{r^3} \right) \cdot \vec{\nabla} V_m \quad (1)$$

where \vec{r} is the distance vector between the measuring point (2.5 μm) and a point in the tissue domain (r is the distance scalar), and $\vec{\nabla}$ denotes the gradient operator. Computed electrograms were stored for its latter processing at a sampling frequency of 1 KHz.

Finally, random electrograms (white noise) were also generated to validate the proposed the proposed methodology in the absence of causality relations among the signals.

2.2. Optical mapping recordings

The optical data was obtained from an isolated Langerdoff-perfused heart. A 14-bit-CCD camera was directed toward a 2x2 cm area of the ventricle and 2 optical fibers connected to a laser served as illumination at 532 nm. Fifteen 5-second movies were recorded at a sampling frequency of 400 Hz, with a resolution of 80x80 pixels. These movies were background subtracted and spatio-temporally filtered using averaging with temporal and spatial windows of 3 ms and 5 pixels. Three movies were recorded during ventricular pacing. Four movies were recorded while the heart was fibrillating, and the last eight movies were recorded after an injection of potassium (4-10 mM) which increases action potential duration and as a consequence increases the organization of the fibrillatory process [4].

3. Methods

Causal relations were searched between neighboring signals placed on a uniform orthogonal mesh. Signals were divided into overlapping segments of length equal to the inverse of the dominant frequency. The autoregressive model (ARM) and surrogate data testing were used to assess causal relationships between signal sections of neighboring nodes. Results were summarized into a causal relation map (CRM) and an organization index (OI).

3.1. Autoregressive modeling

Each pair of simultaneous observations $x_i(t)$ and $x_j(t)$ obtained from neighboring nodes, is assumed to be represented by an:

$$x_i(t) = \sum_{\tau=t_{\min}}^{t_{\max}} a_{\tau} \cdot x_j(t - \tau) + \varepsilon_{ij}(t) \quad (2)$$

where a_{τ} are the ARM coefficients and $\varepsilon_{ij}(t)$ is the error in the prediction of x_i from x_j by using the model, which can be assumed to be a white noise process characterized by its variance $\sigma_{\varepsilon_{ij}}^2$. The order of the ARM model is given by $t_{\max}-t_{\min}$, where $t_{\min} = d/v_{\max}$, $t_{\max} = d/v_{\min}$, d is the distance between nodes, and v_{\max} and v_{\min} are the maximum and minimum conduction velocities respectively, defined as the physiological maximum and minimum conduction velocities in heart tissue. ARM coefficients are estimated by using the least-squares method.

3.2. Surrogate data testing

The noise variance σ_{ε}^2 produced by applying the model ARM was used to assess the degree of causality between two signals since large variances can be

attributed to a weak dependency between source and destiny signals. However, in order to compare on equal terms the degree of causality between different signals with inherent differences in their variance, we used a statistical approach based on surrogate data testing [5].

The method of surrogate data relies on computing the variance of the errors of estimation both on the source signal $x_{source}(t)$ and on a set of surrogate signals $y_s(t)$; $s = 1, \dots, nS$, where nS is the number of surrogate signals created. These surrogate signals are random signals with the same power spectral density than x_{source} and are obtained as follows:

$$y_s = FT^{-1}(|FT(x_i)|e^{j\angle FT(\hat{x}_s)}) \quad (3)$$

where FT and FT^{-1} are the direct and inverse Fourier transform operators respectively, \angle and $|\cdot|$ represent the phase and the modulus operator and \hat{x}_s is a white noise realization of the same length of x_{source} .

We define the Noise to Statistical Threshold Ratio (NSTR), computed for a given pair of signals (i,j) and time frame k , as the ratio between variances of the error of ARM models for the source signal ($\sigma_{\varepsilon_{ij}}^2$) and its surrogates ($\sigma_{\varepsilon_{is}}^2$):

$$NSTR_{ij,k} = \frac{\sigma_{\varepsilon_{is}}^2}{\sigma_{\varepsilon_{ij}}^2} \quad (4)$$

where $\sigma_{\varepsilon_{is}}^2$ is computed as the p percentile of the set nS variances computed for all generated surrogates. The number of surrogates nS was set to 100 and p to 5%.

3.3. Causal relations map and organization index

The result of the proposed method is summarized in a Causal Relation Map, which defines the pattern of signal propagation between different nodes. The CRM is constituted by a vector \vec{v}_i computed for each node, which reflects the direction and intensity of causal relation in that node. This vector is calculated as follows:

$$\vec{v}_i = \frac{1}{nK} \sum_{k=1}^{nK} \vec{s}_{i,k} \quad (5)$$

$$\vec{s}_{i,k} = \sum_{j=1}^{nJ} NSTR_{ij,k} \cdot \hat{u}_{ij} \quad (6)$$

where nK is the number of time frames evaluated, nJ is the number of neighbors of node i , and $NSTR_{ij,k}$ is computed by applying eq. 4, and \hat{u}_{ij} is the unit vector connecting nodes i and j .

The organization index quantifies the stability of the pattern detected in the CRM throughout the observation period and ranges from 0 to 1.

$$OI_i = \left| \frac{1}{K_n} \sum_{k=1}^{nK} \frac{\vec{s}_{i,k}}{|\vec{s}_{i,k}|} \right| \quad (7)$$

With these local measures, we can build an

organization map, which reflects the degree of organization in each node. The global organization index was computed as a mean of local OIs:

$$OI = \frac{1}{N} \sum_{i=1}^N OI_i \quad (8)$$

where N is the number of nodes.

4. Results

4.1. Mathematical models

Figure 1 shows the results of three representative cases in our database. In the first case, in which only one stable focus was present, the CRM allowed to identify the hierarchical process. Directionality vectors in Fig. 1.1.B present a coordinated propagation pattern from the center towards the periphery. Organization map shows a maximum level throughout the tissue surface, except in the focus area, where it is not possible to determine the propagation direction.

In the second case two different tissues were present emulating left and right atria (LA and RA). LA presented a stable rotor, whereas only some of the left activations were able to propagate to the RA since the effective refractory period of the RA was longer (Fig. 1.2A). As it can be observed in Fig. 1.2.B, CRM allowed to characterize the hierarchical pattern and to identify the origin of the arrhythmia. Organization map shows high values for the entire tissue except for the vortex of the rotor and for the transitional tissue between LA and RA.

The third case shows a pattern of random focal activation, where each wavefront comes from a different node. CRM shows an apparently hierarchical pattern from the central region of the tissue to the borders of it. However, the organization map presents lower rates of organization. Notice that, although the simulated pattern is random, nodes in the periphery present a higher organization index since most wavefronts arrive from inside of the simulated tissue and never from outside.

Organization indexes obtained from mathematical models are summarized in Table 1. Notice that computed OIs are higher for patterns that involve more organization (i.e. focus, rotor) than for those patterns that are more disorganized (i.e. random foci, white noise).

4.2. Optical mapping recordings

Results of the analysis for three optical mapping recordings are depicted in Figure 2. The first case corresponds to a pacing pattern from the bottom left corner. The pattern estimated by the CRM summarized the underlying organized process (see Fig 2.1.B). Estimated OI was 0.7 ± 0.05 . The second case was obtained during disorganized ventricular fibrillation. In this case a chaotic pattern was obtained with an OI of

0.27 ± 0.03 . The third illustrated case corresponds to the injection of potassium. CMR (Fig. 2.3.B) showed a more organized pattern than for the case 2, which is corroborated by a higher OI (i.e. 0.44 ± 0.04).

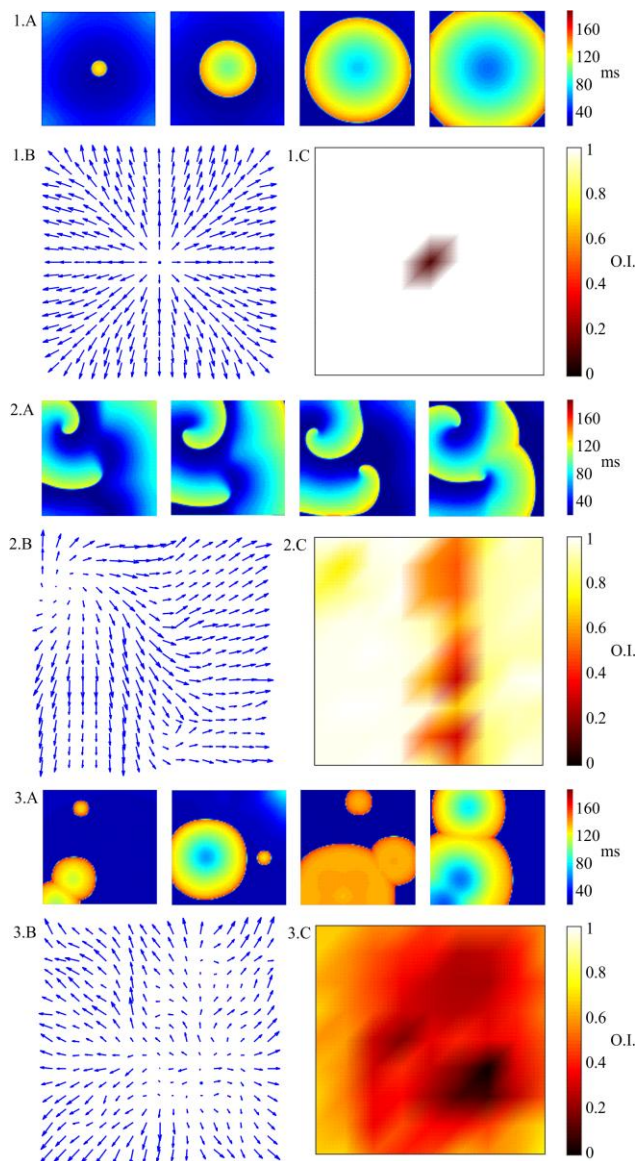


Figure 1. Consecutive images of the activation front (A), CRM (B) and OI map (C) from mathematical models: (1) focal propagation; (2) rotatory propagation in non-uniform tissue; (3) random focal propagation.

Table 1. Organization Indexes (OI) from mathematical models.

Propagation Pattern	O.I.
Focus	0.99 ± 0.09
Rotor	0.98 ± 0.05
Rotor in no uniform tissue	0.87 ± 0.17
Random foci	0.45 ± 0.16
White noise	0.11 ± 0.04

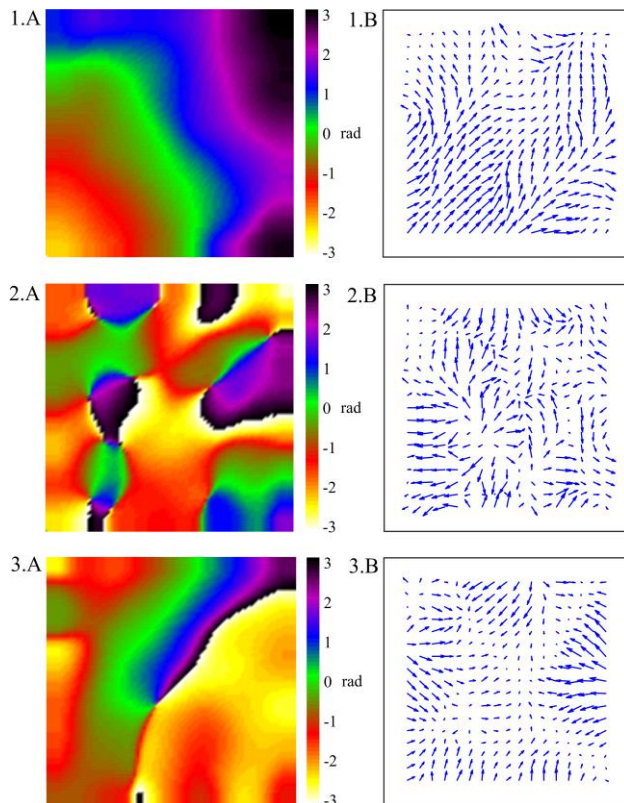


Figure 2. Phase Map (A) and CRM (B) from Optical Mapping signals: (1) during pacing; (2) during fibrillation; (3) during potassium injection.

5. Discussion

This paper presents a novel methodology to identify a possible hierarchical pattern of the myocardial electrical activity during fibrillatory processes. The Causal Relation Map summarizes the electrical activity of a tissue over a period of time, and may be useful to locate areas of the myocardium responsible for the initiation or maintenance of the arrhythmia. In addition, the presented methodology allows the evaluation of the complexity of an obtained pattern by measuring the organization degree of a signal sequence.

In this study, mathematical simulations were used to validate the ability of CRM to identify hierarchical patterns. In addition, optical mapping recordings were used to illustrate the ability of the methodology to estimate the degree of organization of fibrillatory processes.

The mechanisms of fibrillation have been explained by different theories over the studio of the disease: propagation of various wave fronts, reentry circuits or rotatory or focal propagation patterns [1]. However, only recently, clinical studies have demonstrated the ability of the ablation technique to terminate the fibrillation in cases in which the patient presented an activation frequency

gradient [1-3]. In those patients, a small region of the atria triggers the fibrillatory conduction in the rest of the atria. Therefore, having a process to identify whether a hierarchical propagation pattern underlies the electrical activation during fibrillation and to locate the source responsible for its maintenance in each patient may help in increasing the success of the ablation therapy. By using this technique researchers and clinicians could identify the existence of hierarchical patterns and organized activations with a quick look.

Acknowledgements

This research was supported by Spanish Ministry of Education and Science under the project TEC2009-13939 and by the Universitat Politecnica de Valencia through its research initiative program.

References

- [1] Jalife J. Déjà vu in the theories of atrial fibrillation dynamics. *Cardiovasc Res.* 2011 Mar 1;89(4):766-75
- [2] Sanders P, Berenfeld O, Hocini M, Jaïs P, Vaidyanathan R, Hsu LF, Garrigue S, Takahashi Y, Rotter M, Sacher F, Scavée C, Ploutz-Snyder R, Jalife J, Haïssaguerre M. Spectral analysis identifies sites of high-frequency activity maintaining atrial fibrillation in humans. *Circulation.* 2005 Aug 9;112(6):789-97
- [3] Atienza F, Almendral J, Jalife J, Zlochiver S, Ploutz-Snyder R, Torrecilla EG, Arenal A, Kalifa J, Fernández-Avilés F, Berenfeld O. Real-time dominant frequency mapping and ablation of dominant frequency sites in atrial fibrillation with left-to-right frequency gradients predicts long-term maintenance of sinus rhythm. *Heart Rhythm.* 2009 Jan;6(1):33-40.
- [4] Pandit SV, Warren M, Mironov S, Tolkacheva EG, Kalifa J, Berenfeld O, Jalife J. Mechanisms underlying the antifibrillatory action of hyperkalemia in Guinea pig hearts. *Biophys J.* 2010 May 19;98(10):2091-101.
- [5] Richter U, Faes L, Cristoforetti A, Masè M, Ravelli F, Stridh M, Sörnmo L. A novel approach to propagation pattern analysis in intracardiac atrial fibrillation signals. *Ann Biomed Eng.* 2011 Jan;39(1):310-23

Address for correspondence.

M. Rodrigo

*BioITACA, Universitat Politecnica de Valencia,
camino de vera, s.n. 46022, Valencia, Spain
mirodbor@teleco.upv.es*